Aarash Sofla
Department of Mechanical and Aerospace Engineering,
University of Virginia,
Charlottesville, VA 22904

Erkin Seker

James P. Landers

Department of Chemistry,
University of Virginia,
Charlottesville, VA 22904;
Center for Microsystems in the Life Sciences,
University of Virginia,
Charlottesville, VA 22904

Matthew R. Begley[1]
Department of Mechanical and Aerospace Engineering and Department of Materials Science and Engineering,
University of Virginia,
Charlottesville, VA 22904;
Center for Microsystems in the Life Sciences,
University of Virginia,
Charlottesville, VA 22904
e-mail: begley@virginia.edu

PDMS-Glass Interface Adhesion Energy Determined Via Comprehensive Solutions for Thin Film Bulge/Blister Tests

This paper provides comprehensive relationships for pressure, deflection, energy release rate, and phase angle for bulge testing, which are valid for all combinations of the testing length-scales (film thickness, debond size, and bulge height) and materials. These solutions can be used to design experiments that vary relative contributions of opening and sliding displacements at the crack tip by modulating the film thickness, debond size, and bulge volume. Their closed-form nature greatly facilitates property extraction via regression, e.g., modulus from experimental pressure/deflection data or interface toughness from debond size/injected volume data. This is illustrated using experiments to quantify the interfacial adhesion energy between an initially dry polydimethylsiloxane-glass interface via bulge testing under controlled volume injection. The results indicate that the mode-mixity has no effect on the energy required for debonding, which suggests that wetting of the crack faces behind the debonding front eliminates friction.
[DOI: 10.1115/1.4000428]

Keywords: interface adhesion, mode-mixity, bulge testing, PDMS

1 Introduction

Relatively weak, reversible adhesion between soft films and comparatively rigid substrates is widely exploited in many applications, notably microfluidics. In order to design components based on controlled debonding, the relevant interfacial adhesion energy must be known as a function of the relative contributions of interface opening and sliding displacements near the crack tip [1,2]. Bulge testing allows different combinations of crack tip sliding and opening to be probed by varying the testing length-scales, i.e., the film thickness, bulge height, and size of the debonded region [1–4] (see Fig. 1). Controlled volume injection leads to stable debonding, and facilitates the study of the role of fluids in altering crack advance mechanisms [5]. Perhaps most importantly, the test can be easily interpreted using established mixed-mode fracture mechanics models, which can be used to extract mixed-mode interface properties that can be applied to other geometries in a clear manner.

A significant practical difficulty when extracting material properties from bulge testing is that the scaling between relevant variables (e.g., deflection and pressure) change dramatically as a function of film thickness, bulge radius, and deflection. In a nutshell, one transitions from classical plate mechanics to classical membrane solutions for large deflections. Although numerical solutions for these limits and associated transitions are ubiquitous (e.g., see [6] and references therein), they often do not include closed-form relationships that can be fitted to experiments. Most importantly, previous works do not present sufficient information to extract the mode-mixity and energy release rate to predict debonding for arbitrary deflections. The plate and membrane limits are well covered, as are numerical results illustrating transitions for a few select example cases [1–4]. In order to predict the relevant fracture parameters, the resultant moment and normal loads must be known as a function of film deflection across the entire range of the test. Closed-form expressions are critical for efficient property extraction; even with complicated functions, such fits can be achieved with a single line in modern computational tools such as MATHEMATICA [7].

Here, we present comprehensive closed-form solutions that fully describe bulging and debonding behaviors across the full range of length-scales (film thickness, debond size, and bulge height), i.e., compact expressions that span the entire regime from plate to membrane behavior. These solutions enable straightforward extraction of film properties, including mixed-mode fracture properties. To illustrate their utility, they are used to quantify the interfacial adhesion energy between initially dry glass and polydimethylsiloxane (PDMS), which is a material combination prevalent in microfluidics. The tests and associated theory illustrate that

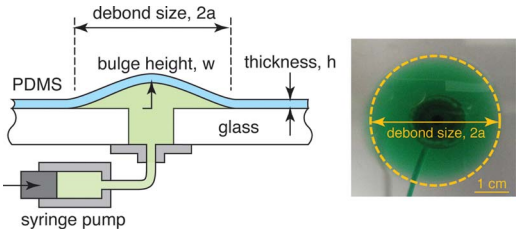

Fig. 1 Schematic illustration of the bulge test and representative image of the delamination front during a blister test on PDMS. The debond radius is estimated by fitting a curve to the edge of the region where the dyed fluid is visible.

[1]Corresponding author.

Contributed by the Applied Mechanics Division of ASME for publication in the JOURNAL OF APPLIED MECHANICS. Manuscript received March 7, 2009; final manuscript received September 24, 2009; published online February 4, 2010. Assoc. Editor: Robert M. McMeeking.

Table 1 Interpolation functions for fundamental variables of blister test

Deflection, $\bar{\delta}$	$\frac{\bar{P}}{1+d(v)\bar{P}^2}+\exp\left(\frac{-(2-1.9v)}{\bar{P}}\right)\left(\frac{50\bar{P}}{23+18v-3v^2}\right)^{1/3}$	$d(v)=0.669+0.809v+3.068v^2$
Moment, $\bar{M}$	$\left(\frac{2}{3}\right)\bar{\delta}+\left[\frac{m(v)\bar{\delta}^{1.25}}{(2.2+\bar{\delta}^{1.25})}\right]\bar{\delta}^2$	$m(v)=0.509+0.221v-0.263v^2$
Normal, $\bar{N}$	$n(v)(-0.255\bar{\delta}^2\exp(-0.16\bar{\delta}^{1.3})+0.667\bar{\delta}^2)$	$n(v)=0.809-1.073v-0.816v^2$

it is possible to probe mode-mixity phase angles in the range of -45 deg to -70 deg, simply by varying the film thickness such that the test spans the plate to membrane transition. As illustrated here, it is critical in such tests to have complete solutions for arbitrary deflections to extract material parameters.

2 Thin Film Mechanics

The behavior of a pressurized, linearly elastic circular film can be completely described in terms of the following dimensionless variables, regardless of the level of deformation [3,6]

$$\bar{\delta}(\bar{P},\nu)=\frac{\delta}{h},\quad \bar{P}=\frac{3pa^4}{16\bar{E}h^4},\quad \bar{M}(\bar{\delta},\upsilon)=\frac{a^2M}{\bar{E}h^4},\quad \bar{N}(\bar{\delta},\upsilon)=\frac{a^2N}{\bar{E}h^4} \tag{1}$$

where δ is the center-point deflection, p is the applied pressure, h is the film thickness, and $\bar{E}=E/(1-\upsilon^2)$ is the plane strain elastic modulus (where υ is the Poisson's ratio of the film). The normalized load is chosen such that for small deformation (i.e., the plate limit), $\bar{\delta}=\bar{P}$. The membrane resultant N has units of force (i.e., not the resultant per unit thickness of the film), while M represents the moment per unit length in the circumferential direction (i.e., has units of force). Dimensionless governing equations can be written completely in terms of $(\bar{M},\bar{N})$; however, the boundary condition at the clamped edge involves the Poisson's ratio, and hence, any solution describing the relationships $\bar{\delta}(\bar{P})$, $\bar{M}(\bar{\delta})$, and $\bar{N}(\bar{\delta})$ is only strictly applicable for a specific value of υ, despite its presence in the above normalizations.

Finite element analyses were conducted for a single geometry (i.e., film thickness and radius), a single modulus, and $\upsilon=0$, 1/4, and 1/2, to determine the center-point deflection and resultant moments and normal forces at the clamped edge as a function of pressure. The results were normalized according to the above description; since the govern equations can be completely described in terms of these normalized variables, the results represent universal solutions for a specified υ and any thickness, radius, and modulus. The numerical relationships describing $\bar{\delta}(\bar{P},\upsilon)$, $\bar{M}(\bar{\delta},\upsilon)$, and $\bar{N}(\bar{\delta},\upsilon)$ were fit with closed-form approximations that represent interpolations between the asymptotic solutions for plate ($\bar{\delta}\ll 1$) and membrane behaviors ($\bar{\delta}\gg 1$). That is, the general form of the approximations is

$$u(\bar{\delta})=f_1(\bar{\delta},\upsilon)u_p(\bar{\delta})+f_2(\bar{\delta},\upsilon)u_m(\bar{\delta}) \tag{2}$$

where $u_p(\bar{\delta})$ and $u_m(\bar{\delta})$ are the asymptotic limits for the variable u in the plate and membrane limits (respectively, if available), and $f_i(\bar{\delta},\upsilon)$ are interpolation functions that capture the transition from plate to membrane behavior. The latter functions are chosen such that $\lim_{\bar{\delta}\to 0}f_1(\bar{\delta},\upsilon)=1$, $\lim_{\bar{\delta}\to\infty}f_1(\bar{\delta},\upsilon)=0$, $\lim_{\bar{\delta}\to 0}f_2(\bar{\delta},\upsilon)=0$, and $\lim_{\bar{\delta}\to\infty}f_2(\bar{\delta},\upsilon)=1$. Hence, the approximations are asymptotically exact for large and small deflections.

The interpolation functions for the core variables in the analysis are given in Table 1. Fitting constants in the interpolation functions were determined via regression using MATHEMATICA. A comparison of the numerical results and fits is shown in Fig. 2, along with the percent errors in the fits (as determined by comparing

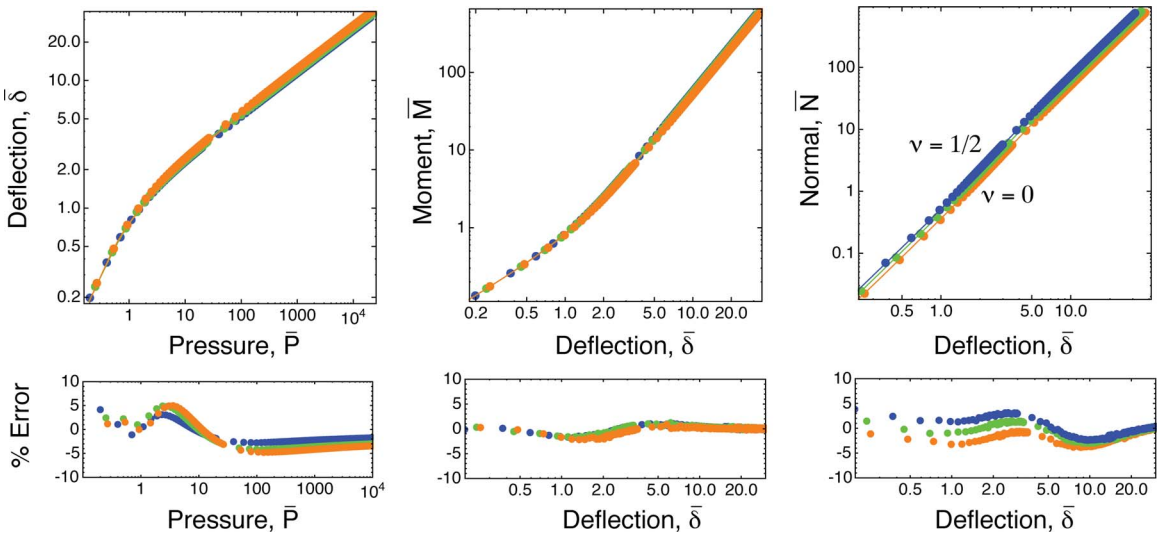

Fig. 2 Illustration of the basic relationships between normalized variables, the fitted interpolation functions, and relative error, for $\upsilon=0$, 1/4, and 1/2. Differences due to Poisson's ratio are subtle, but strongly influence mode-mixity during debonding.

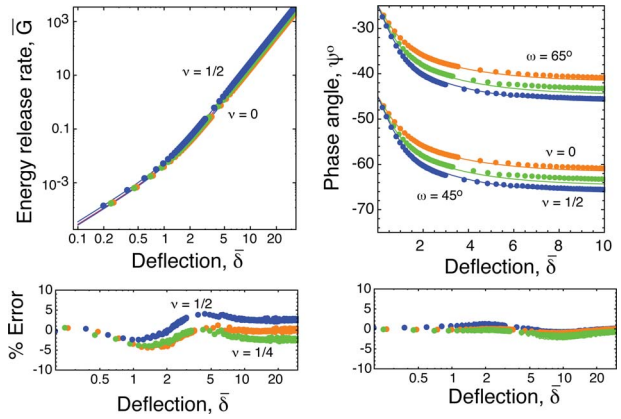

Fig. 3 The interface debonding parameters as a function of deflection for several material parameters, and the relative error between values computed via raw numerical data and those computed using interpolation functions

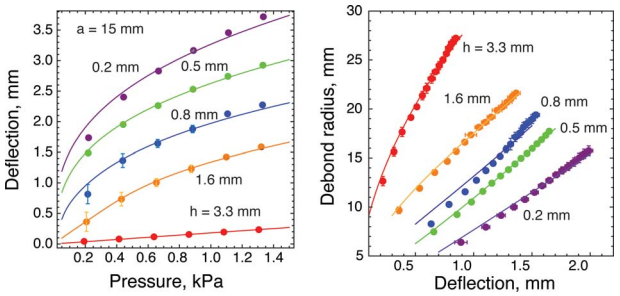

Fig. 4 Experimental results for aqueous injection: (*a*) deflection versus pressure (used to determine modulus), and (*b*) debond radius versus deflection (used to determine interface toughness). Points without error bars have smaller deviations than the plotting symbols.

predictions and numerical results at specific points generated by the finite element analysis). Each fit has less than 5% error over the entire range. Despite the obvious similarities in the results, there is no obvious universally applicable form for the interpolation functions; hence, the rather unusual and different interpolation functions for each variable. While the effects of Poisson's ratio appear subtle when illustrated on a log-log scale, ignoring its effect (i.e., treating the results in Fig. 2 as independent of Poisson's ratio) leads to substantial errors. It is also interesting to note that the normal resultants, although appearing to scale as $\bar{N} \propto \bar{\delta}^2$, have very subtle variations from this scaling for small deflections. While these subtle variations have no relative impact on the energy release rate for small deflections (i.e., in the plate limit, as expected), they strongly influence the mode-mixity involved in debonding, which is detailed next.

3 Interface Delamination Mechanics

The energy release rate and mode-mixity controlling debonding at the outer edge of the circular film can be written entirely in terms of the normalized variables detailed above. The appropriate normalized relations for the energy release rate G and phase angle ψ are [1–4]

$$\bar{G}(\bar{\delta},\upsilon) = \bar{G}(\bar{M},\bar{N}) = \frac{a^4 G}{\bar{E}h^5} = \frac{1}{2}(12\bar{M}^2 + \bar{N}^2) \tag{3}$$

and

$$\tan\psi = \frac{\sqrt{12}\bar{M}\cos\omega + \bar{N}\sin\omega}{-\sqrt{12}\bar{M}\sin\omega + \bar{N}\cos\omega} \tag{4}$$

where $\omega(\alpha) = 52.1^0 + 8.691^0\alpha + 6.45^0\alpha^2 + 4.893^0\alpha^3$, and α is the first of Dundur's parameters [1]. This phase-angle relationship is only valid for cases where the second of Dundur's parameters is approximately zero [1,2]. For cases with extreme stiffness mismatch (e.g., elastomers on pretty much any substrate, or glassy polymers on ceramics or metal substrates), $\alpha \simeq -1$ and $\omega \simeq \pi/4 = 45$ deg.

Figure 3 illustrates the energy release rate and mode-mixity (for two values of ω) as a function of center-point deflection for $\upsilon = 0$, ¼, and 1/2. The data points reflect computations using the raw data from the finite element analysis, while the lines reflect the result using the interpolation functions. The percentage difference between these two methods is also shown to evaluate the effect of interpolation errors as they trickle through the computation. The results in Fig. 3 illustrate that the largest changes in mode-mixity occur for small deflections, where the normal result is small and contributes little to the overall energy release rate. This illustrates the importance of accurate interpolation functions for the normal resultant at small deflections.

The mixed-mode interface adhesion energy G_c is determined by setting $G = G_c$ in Eq. (3) and fitting the resulting expression for $a = f(G_c, \delta)$ to the experimental result. The influence of mode-mixity is often described in terms of a mixed-mode interface adhesion energy, i.e., $G_c(\psi) = G_{Ic}(1 + \tan^2[\eta\psi])$, where η is an experimentally determined parameter controlling the influence of mode-mixity [1,2]. This expression can be used with the equations above to capture the possible influence of changing mode-mixity during debonding, i.e., $a = f(G_c, \eta, \delta)$.

4 PDMS-Glass Adhesion Energy: Application of the Comprehensive Solutions

The schematic shown in Fig. 1 illustrates the essential elements of the experimental approach. PDMS films (HT 6240 from Bisco® silicone) of various thickness were laid on top of a glass plate, which contained a hole connected to a fluid source. The height of the bulge was measured using extrinsic Fabry–Perot interferometry (EFPI) (Fiberpro USB from Luna Innovation, Raonoke, VA), while images of the debonded region were simultaneously acquired with a high resolution digital camera. Food color dye was added to deionized water to improve the optical contrast at the edge of the debonded region. To measure the modulus of each film, the size of the bulge was fixed by clamping a plate with a 15-mm radius hole; the fluid source was raised to different heights to impose the hydrostatic pressure on the film, and the resulting bulge height was recorded. For the adhesion tests, a syringe pump (3 ml from BD Syringe with SP100i infusion pump from WPI, Inc., Sarasota, FL) was used to inject controlled volumes; optical images of the debonding front and EFPI deflection measurements were obtained for volumes ranging from 0.05–0.75 ml. Three types of each test (modulus and adhesion) were conducted for each film thickness. Between each test, the film was removed; the glass surface was then cleaned with Piranha solution and both surfaces subsequently dried with nitrogen. Images acquired immediately after the injection were used to calculate the debond radius by digitally imposing an ellipse over the image at the edge of contrast. In all instances, the circular debond had less than 10% eccentricity. Tests were conducted at various injection rates to determine that there were no rate-effects observed for the debonding process; there was less than several percent difference in debond radius for volume injection rates ranging from 5 ml/h to 25 ml/h. An injection rate of 10 ml/h was used for the present experiments.

Figure 4 shows the results of the pressure-deflection tests (used to extract film modulus) and the debonding tests (use to extract interfacial adhesion energy). The data points and error bars indicate the average and standard deviation from three separate tests;

Table 2 Experimentally determined properties of the PDMS-glass system

Thickness $\langle x\rangle \pm \sigma$ (mm)	Modulus $\langle x\rangle \pm \sigma$ (MPa)	Adhesion energy $\langle x\rangle \pm \sigma$ (J/m^2)	Test range of phase angles $\psi^0_{max}, \psi^0_{min}$
$\langle 0.231\rangle \pm 0.003$	$\langle 1.412\rangle \pm 0.016$	$\langle 0.197\rangle \pm 0.024$	−65.9, −63.2
$\langle 0.487\rangle \pm 0.003$	$\langle 1.256\rangle \pm 0.027$	$\langle 0.106\rangle \pm 0.004$	−62.5, −57.0
$\langle 0.814\rangle \pm 0.008$	$\langle 1.462\rangle \pm 0.194$	$\langle 0.139\rangle \pm 0.016$	−59.3, −53.3
$\langle 1.569\rangle \pm 0.016$	$\langle 0.966\rangle \pm 0.003$	$\langle 0.132\rangle \pm 0.012$	−54.0, −47.7
$\langle 3.390\rangle \pm 0.015$	$\langle 1.005\rangle \pm 0.017$	$\langle 0.152\rangle \pm 0.016$	−47.9, −45.8

where they are not visible, they are smaller than the plot markers. The modulus of each film was determined by fitting the relevant equation in Table 1 to each individual pressure-deflection data set, with E as the single fitting parameter (assuming $\nu=1/2$). The average modulus and standard deviation from the values from fitting each test are given in Table 2. The lines in Fig. 4 represent the interpolation predictions using the average value of E. The comparatively poor fit and high modulus of the thinnest film ($h=0.231$ mm) is likely a consequence of the difficulties of bonding thin films without prestrain, and of accurately determining a reference deflection that corresponds to the zero strain. Fitting the last few data points (i.e., neglecting the data for smaller deflections, as they are more influenced by initial conditions) predicts $E\sim 1.2$ MPa.

Figure 4 shows the results of the debonding tests; the interface adhesion energy was determined by fitting the relevant result in Table 1 to the data, with $G=G_c$ as the only fitting constant. That is, the experimental values of modulus and thickness were used. The average interface adhesion energy and standard deviations obtained from three tests are given in Table 1. Again, these values are determined from the data sets obtained by fitting each individual experiment (as opposed to fitting the average for all experiments). The range of mode-mixity that is probed in each test is illustrated in Fig. 5, as determined by plugging the measured deflections into the expressions listed above for mode-mixity. As indicated by the results in Fig. 5, the chosen length-scales effectively probe the entire range of possible phase angles for a blister test, with relatively little overlap from one thickness to the next.

The results strongly suggest there is negligible mode-dependence of the adhesion energy, since comparable adhesion energies are obtained regardless of the phase angle probed in each test. The comparatively high result for the thinnest film may be a result of the high modulus value, since the predicted G scales with the modulus. In the context of mixed-mode fracture mechanics, this implies the interface is "ideally brittle," since debonding is independent of the relative amount of sliding at the interface.

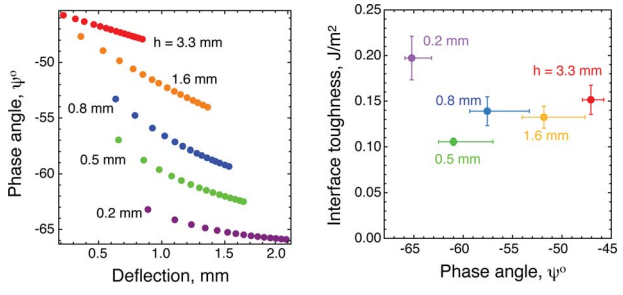

Fig. 5 Predictions of the phase angles for each test as a function of experimentally measured deflection, and the interface toughness implied by curve fitting to the results in Fig. 4. The error bars on the toughness reflect the standard deviation from three measurements, while the error bars on the phase angle reflect the range probed during the test.

The nominal value of $G_c\sim 0.1-0.2$ J/m^2 is in strong agreement with sperical indentation tests on PDMS-glass interfaces [8] and 40 deg peel tests *at low velocity* conducted on PDMS-PDMS interfaces [9]. In the latter study of steady-state debonding under fixed load, the authors demonstrate that frictional sliding in the debonding zone strongly influences the macroscopically observed adhesion energy, and is a strong function of peel angle (see Figure 10 in Ref. [8], i.e., at low velocities on the order of 50 μm/s, $G_c\sim 0.2$ J/m^2 for 40 deg peel ($\psi\sim -55$ deg) and $G_c\sim 3$ J/m^2 for 5 deg peel ($\psi\sim -85$ deg)). Obviously, distinction must be made between steady-state crack advance (under fixed load) and initiation (under fixed displacement). Moreover, the steady-state debonding study in Ref. [8] involved a monolayer of PDMS on the glass surface, which may increase the role of frictional sliding over the present study.

Even if a dissipation mechanism (either viscoelasticty or frictional sliding) were possible, the present results suggest that lubrication of the crack faces behind the debonding zone eliminates frictional dissipation and washes out mode-mixity effects. This implies the liquid-injection approach offers the opportunity to separate the effects of friction and rate-effects associated with material deformation. Naturally, the latter depends on the strength of the interface; in the present case, it seems clear that the bond strength of PDMS-glass interface is not sufficient to generate significant inelastic shielding (as manifested by strong mode-mixity effects). Interestingly, the present results are consistent with fixed load peel tests on ethylene propylene rubber-glass interface [10], which showed no mode-mixity effects for peel angles ranging from 15 deg to −90 deg (ψ from −85 deg to −45 deg). Presumably, the large observed adhesion energy (~ 5 J/m^2) for this rubber-glass system was dominated by chemical bonding (as opposed to friction), and the mechanisms associated with debond initiation did not trigger rate-dependent material response that would lead to mode-mixity effects.

5 Concluding Remarks

For many thin film systems, it is difficult to design a bulge test that lies entirely in either the plate or membrane regimes; the present solutions overcome this difficulty by providing accurate closed-form results that span the entire range of deflection. As is well known, the mode-mixity of the delamination in blister delamination is sensitive to the deflection, spanning the entire possible range for deflections on the order of several film thickness. Moreover, the mode-mixity is quite sensitive to the elastic properties of the system. The present solutions circumvent the need to interpolate between example cases in previous work, as well as the need to conduct a variety of numerical analysis to capture relationships between experimental variables.

With regard to PDMS-glass adhesion, the present example provides a clear, precise treatment of mode-mixity effects, and confirms that the relative contributions of sliding and bending are unimportant—at least, for the lubricated tensile interfaces most relevant to microfluidics. On one hand, this lack of mode-mixity effects for weakly bonded PDMS-glass systems has fortunate implications for microfluidic applications, since interface stability can be predicted based on straightforward calculations of energy release rate without concern over more complicated calculation of mode-mixity [6]. On the other hand, the results imply that debonding initiated by a critical pressure will not arrest; changes in the phase angle as the debond advances will not inhibit growth, unlike other systems with strong mixity effects caused by inelastic shielding mechanisms, including frictional sliding.

Acknowledgment

The authors gratefully acknowledge the support of the National Science Foundation through Grant No. CMII0800790.

References

[1] Hutchinson, J. W., and Suo, Z., 1991, "Mixed-Mode Cracking in Layered Materials," Adv. Appl. Mech., **29**, pp. 63–161.

[2] Freund, L. B., and Suresh, S., 2003, *Thin Film Materials*, Cambridge University Press, Cambridge, England.

[3] Jensen, H. M., 1998, "Analysis of Mode Mixity in Blister Tests," Int. J. Fract., **94**, pp. 79–88.

[4] Jensen, H. M., 1991, "The Blister Test for Interface Toughness Measurement," Eng. Fract. Mech., **40**, pp. 475–486.

[5] Begley, M. R., and Monahan, J., 2007, "The Mechanical Behavior of Films and Interfaces in Microfluidic Devices: Implications for Performance and Reliability," *CRC Handbook of Microcapillary Electrophoresis*, CRC, Boca Raton, FL, Chap. 39, pp. 1121–1151.

[6] Komaragiri, U., Begley, M. R., and Simmonds, J. G., 2005, "The Mechanical Response of Freestanding Circular Films Under Point and Pressure Loads," ASME J. Appl. Mech., **72**, pp. 203–212.

[7] MATHEMATICA software, www.wolfram.com

[8] Savkoor, A. R., and Briggs, G. A. D., 1977, "The Effect of Tangential Force on the Contact of Elastic Solids in Adhesion," Proc. R. Soc. London, Ser. A, **356**, pp. 103–114.

[9] Newby, B. Z., and Chaudhury, M. K., 1998, "Friction in Adhesion," Langmuir, **14**, pp. 4865–4872.

[10] Kendall, K., 1975, "Thin-Film Peeling—The Elastic Term," J. Phys. D, **8**, pp. 1449–1452.